

Results and Discussion

Synthesis of Peptides The peptides **1** and **4** were synthesized in accordance with the methods outlined in refs. 13 and 14, respectively. The nonapeptides Boc-(L-Leu-L-Leu-Aib)₂-L-Leu-D-Leu-Aib-OMe (**2**) and Boc-L-Leu-D-Leu-Aib-L-Leu-L-Leu-Aib-L-Leu-D-Leu-Aib-OMe (**3**) were synthesized using conventional solution-phase methods involving a fragment condensation strategy in which 1-(3-dimethylaminopropyl)-3-ethylcarbodiimide (EDC) hydrochloride and 1-hydroxybenzotriazole (HOBt) hydrate were employed as coupling reagents. All of the compounds were purified by column chromatography on silica gel.

Conformational Analyses of the Peptides in Solution (Fourier Transform (FT)-IR and Circular Dichroism (CD))

Spectra The IR spectra of peptides **2**, **3** and **4** were measured in the NH-stretching region ($3200\text{--}3500\text{cm}^{-1}$) at a peptide concentration of 2.0mM in CDCl_3 solution. In the spectra of **2**, **3** and **4**, the weak bands in the 3434 and 3439cm^{-1} regions were assigned to solvated free peptide NH groups, and the strong band at 3334cm^{-1} was assigned to peptide NH groups with $\text{N-H}\cdots\text{O}=\text{C}$ intramolecular H-bonds. These spectra were very similar to those of helical peptides in solution.^{3,16} Peptide **1** exhibited similar spectra to peptides **2**, **3** and **4**¹³ (Fig. 2).

The CD spectra of peptides **1–4** were measured in 2,2,2-trifluoroethanol (TFE) and TFE and phosphate buffered saline (PBS) buffer (1:1) solution (peptide concentration: 0.1mM). The spectra of the peptides displayed negative maxima at

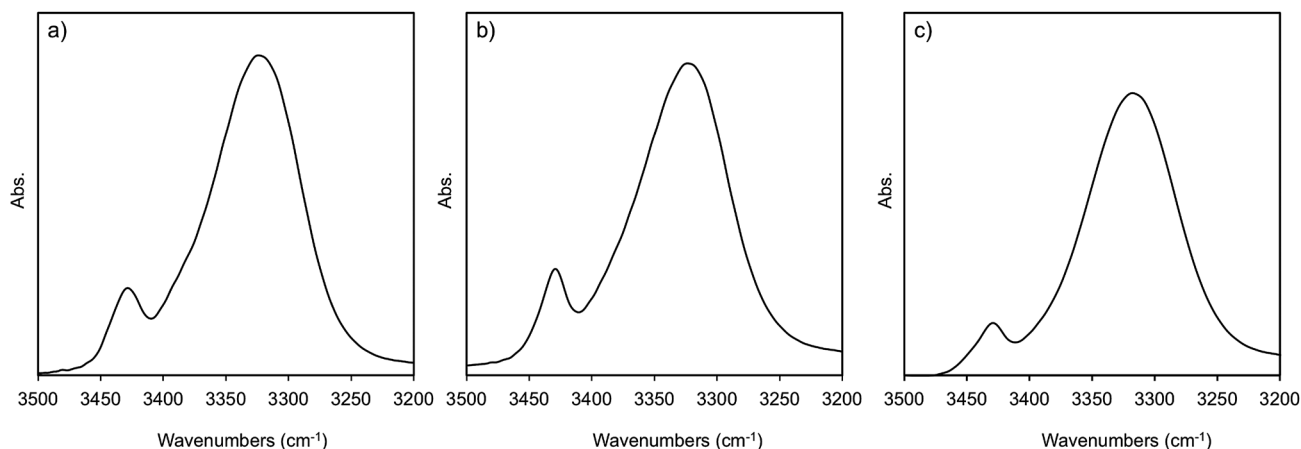


Fig. 2. FT-IR Spectra of Peptides **2** (a), **3** (b) and **4** (c) in CDCl_3 Solution

Peptide concentration: 2.0mM .

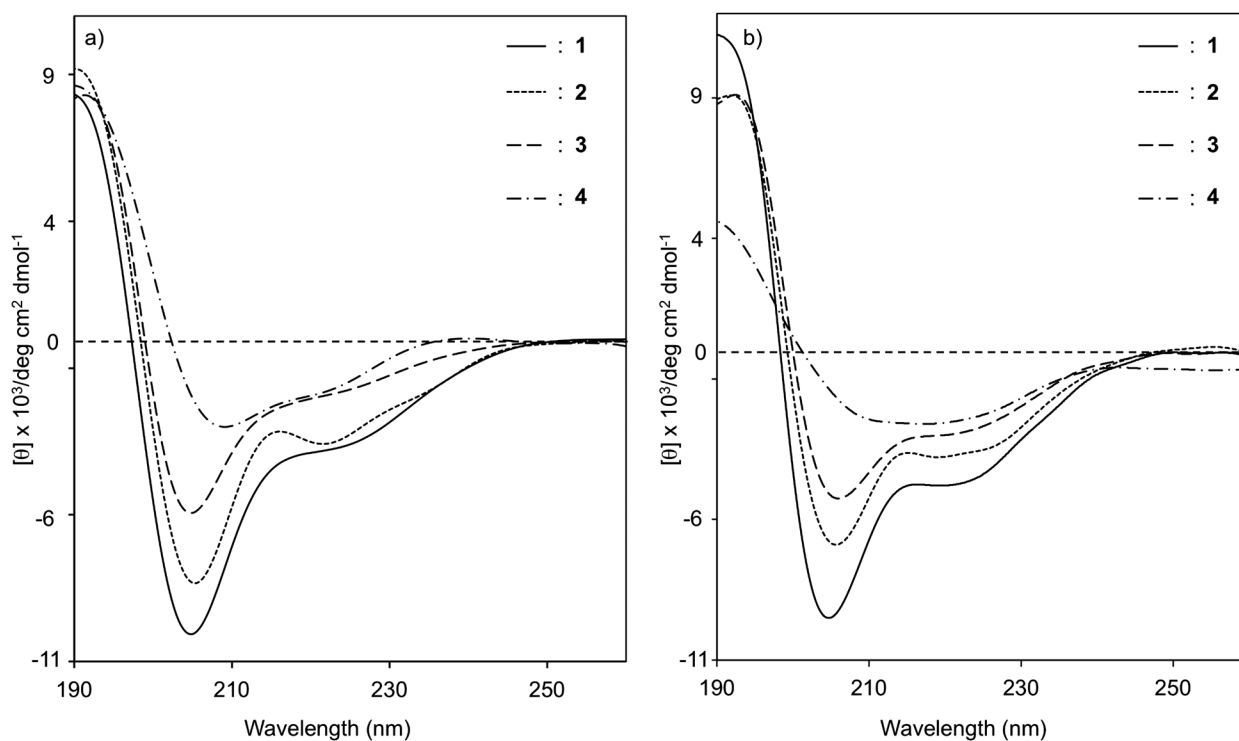


Fig. 3. CD Spectra of Nonapeptides **1–4** in TFE (a) and TFE/PBS (pH 7.2)=1:1 Solution (b)

Peptide concentration: 0.1mM .

Table 1. Crystal and Diffraction Parameters of Peptides **2** and **3**

	2	3
Formula	C ₅₄ H ₉₉ N ₉ O ₁₂ , C ₄ H ₉ NO	C ₅₄ H ₉₉ N ₉ O ₁₂ , CH ₄ O, C ₂ H ₃ N
Crystal dimensions [mm]	0.50×0.40×0.03	0.45×0.30×0.15
Crystal system	Orthorhombic	Orthorhombic
Lattice parameters:		
<i>a</i> [Å]	12.6227	14.7729
<i>b</i> [Å]	13.7970	20.2473
<i>c</i> [Å]	38.891	45.357
<i>α</i> [°]	90	90
<i>β</i> [°]	90	90
<i>γ</i> [°]	90	90
<i>V</i> [Å ³]	6773.0	13567
Spacer group	<i>P</i> 2 ₁ 2 ₁ 2 ₁	<i>P</i> 2 ₁ 2 ₁ 2 ₁
<i>Z</i> value	4	4
<i>D</i> _{calc} [g/cm ³]	1.13	1.08
<i>μ</i> (MoK α) [cm ⁻¹]	0.80	0.86
No. of observations	6824 (<i>I</i> >2 σ (<i>I</i>))	12914 (<i>I</i> >2 σ (<i>I</i>))
No. of variables	730	1399
<i>R</i> ₁ , <i>R</i> _w	0.0561, 0.1566	0.0557, 0.1567
Solvent	DMA/H ₂ O	MeOH/MeCN

around 206 and 224 nm (208 nm and 224 nm for the peptide **4**), indicating that they possessed a right-handed (*P*) helical screw sense, as shown in Fig. 3A.¹²⁾ Based on the *R* values ($\theta_{224}/\theta_{206}$) of the peptides, the homochiral peptide **1** and the heterochiral peptides **2** and **3** formed 3₁₀-helices as their dominant conformations (*R*=0.38 for **1**, *R*=0.44 for **2**, *R*=0.34 for **3**), whereas the LD-peptide **4** preferentially formed an α -helix ($R=\theta_{224}/\theta_{209}=0.71$).¹⁷⁾ Based on the intensity values of the peptides' CD spectra, it was considered that peptide **1**, which is entirely composed of L-Leu residues, formed the most right-handed (*P*) helical structure, and the peptides' CD intensities decreased linearly as the number of D-Leu residues in the nonapeptide sequence increased. Whereas, the peptide **4** having the alternating L-Leu-D-Leu-Aib segment preferentially formed a right-handed (*P*) α -helix rather than a 3₁₀-helix.¹⁵⁾ Thus, as the number of D-Leu residues in a helical L-peptide sequence increased, the right-handed (*P*) 3₁₀-helices are gradually destabilized and tends to change their dominant conformations from 3₁₀-helices to α -helices. Even in a mixture of TFE and PBS buffer (1:1) solution, all peptides formed (*P*) helical structures, respectively, as shown in Fig. 3B.

X-Ray Diffraction Analysis Peptides **2** and **3** produced suitable crystals for X-ray crystallographic analysis after the slow evaporation of *N,N*-dimethylacetamide (DMA)/H₂O and MeOH/MeCN, respectively, at room temperature. The crys-

Table 2. Selected Torsion Angles (ϕ , ψ , ω , and χ) [°] for Peptides **2** and **3**

Residue	Torsion angle			
	ϕ	ψ	ω	χ
Boc-(L-Leu-L-Leu-Aib) ₂ -L-Leu-D-Leu-Aib-OMe (2)				
L-Leu(1)	-53.7	-44.3	-176.1	-178.1
L-Leu(2)	-53.2	-47.1	-177.6	174.7
Aib(3)	-57.7	-42.8	-174.5	—
L-Leu(4)	-77.6	-33.2	172.8	-53.8
L-Leu(5)	-56.7	-43.8	179.0	172.3
Aib(6)	-55.5	-29.8	-178.1	—
L-Leu(7)	-96.2	10.5	172.6	-61.7
D-Leu(8)	92.3	11.9	173.7	62.2
Aib(9)	-48.7	-40.3	174.9	—
Boc-L-Leu-D-Leu-Aib-L-Leu-L-Leu-Aib-L-Leu-D-Leu-Aib-OMe (3)				
Molecule A				
L-Leu(1A)	-64.4	-35.5	-178.4	177.2
D-Leu(2A)	-52.7	-57.4	-178.8	-29.1
Aib(3A)	-57.5	-44.8	-177.0	—
L-Leu(4A)	-60.4	-40.2	177.5	-61.7
L-Leu(5A)	-66.1	-44.1	-178.8	-67.3
Aib(6A)	-54.6	-35.2	-177.5	—
L-Leu(7A)	-86.4	-8.1	-169.8	-66.6
D-Leu(8A)	55.8	39.5	175.2	174.0
Aib(9A)	-54.2	-28.3	176.8	—
Molecule B				
L-Leu(1B)	-66.1	-43.8	-176.6	176.5
D-Leu(2B)	-53.0	-53.6	-178.6	63.7
Aib(3B)	-55.7	-47.1	-176.7	—
L-Leu(4B)	-59.7	-44.4	-177.1	-66.1
L-Leu(5B)	-70.1	-40.0	179.4	-64.1
Aib(6B)	-54.9	-35.2	-177.1	—
L-Leu(7B)	-88.5	-9.5	-170.8	-75.3
D-Leu(8B)	66.0	25.5	169.8	77.4
Aib(9B)	49.8	-136.8	-179.5	—

tal and diffraction parameters of **2** and **3** are summarized in Table 1. Data collection was performed using a Bruker AXS SMART APEX imaging plate diffractometer and graphite-monochromated MoK α radiation. The structures of **2** and **3** were solved by the direct method using SHELXS 97¹⁸⁾ and expanded using the Fourier technique.¹⁹⁾ All non-H atoms were given anisotropic thermal parameters, some H atoms were refined isotropically, and the remaining H atoms were placed at the calculated positions.²⁰⁾ The crystal and diffraction parameters of the peptides, as well as relevant backbone and side chain torsion angles and intra- and intermolecular hydrogen-bond parameters are summarized in Tables 2 and 3.

A right-handed (*P*) α -helix with a dimethylacetamide molecule was existed in the asymmetric unit of Boc-(L-Leu-L-Leu-Aib)₂-L-Leu-D-Leu-Aib-OMe (**2**) (Fig. 4). The mean φ and ψ torsion angles of the amino acid residues (1–6) were -59.1° and -40.2° , respectively, which are close to those of an ideal (*P*) α -helix (-60° and -45° , respectively). However, the D-Leu (8) residue was flipped,^{21,22)} and its φ and ψ torsion angles were positive ($\varphi=+92.3^\circ$, $\psi=+11.9^\circ$). Two $i\leftarrow i+3$ type, two $i\leftarrow i+4$ type, and one $i\leftarrow i+5$ type hydrogen bond were found in the α -helix of **2**. Hydrogen bonds were detected between the H-N(4) and C(0)=O(1) [N(4) \cdots O(0)=3.47 Å; a bit long for a hydrogen bond], between the H-N(5) and C(1)=O(1) [N(5) \cdots O(1)=2.91 Å], between the H-N(6) and C(2)=O(2) [N(6) \cdots O(2)=3.20 Å], between the H-N(7) and C(4)=O(4) [N(7) \cdots O(4)=3.01 Å], between the H-N(8) and C(5)=O(5) [N(8) \cdots O(5)=2.89 Å], and between the H-N(9) and C(4)=O(4)

[N(9) \cdots O(4)=3.01 Å]. In packing mode, successive helical molecules were connected by an intermolecular hydrogen bond to form head-to-tail aligned chains.

The asymmetric unit of Boc-L-Leu-D-Leu-Aib-L-Leu-L-Leu-Aib-L-Leu-D-Leu-Aib-OMe (**3**) contained two right-handed (*P*) α -helical structures, in which the D-Leu (8) residue was flipped (Fig. 5). The conformations of molecules **A** and **B** were well matched, except for small differences in the conformations of their side chains and C-terminus peptide backbones (Fig. 6). The mean φ and ψ torsion angles of the α -helical residues (1–7) were -59.3° and -42.9° , respectively, for **A**, and -59.9° and -44.0° , respectively, for **B**. Regarding the intramolecular H-bonds in molecule **A**, one $i\leftarrow i+3$ type, four $i\leftarrow i+4$ type, and one $i\leftarrow i+5$ type hydrogen bond were formed. The hydrogen bonds were located between the H-N(4a) and C(0a)=O(0a) [N(4a) \cdots O(0a)=3.14 Å], between the H-N(5a) and C(1a)=O(1a) [N(5a) \cdots O(1a)=2.89 Å], between the H-N(6a) and C(2a)=O(2a) [N(6a) \cdots O(2a)=3.09 Å], between the H-N(7a) and C(3a)=O(3a) [N(7a) \cdots O(3a)=3.18 Å], between the H-N(8a) and C(5a)=O(5a) [N(8a) \cdots O(5a)=2.94 Å], and between the H-N(9a) and C(4a)=O(4a) [N(9a) \cdots O(4a)=2.93 Å]. In molecule **B**, the same types of H-bonds as shown in molecule **A**, were detected between the H-N(4b) and C(0b)=O(0b) [N(4b) \cdots O(0b)=3.25 Å], between the H-N(5b) and C(1b)=O(1b) [N(5b) \cdots O(1b)=2.95 Å], between the H-N(6b) and C(2b)=O(2b) [N(6b) \cdots O(2b)=3.02 Å], between the H-N(7b) and C(3b)=O(3b) [N(7b) \cdots O(3b)=3.31 Å; a bit long for a H-bond], between the H-N(8b) and C(5b)=O(5b)

Table 3. Intra- and Intermolecular H-Bond Parameters for Peptides **2** and **3**

Peptide ^{a)}	Donor D–H	Acceptor A	Distance [Å] D \cdots A	Angle [°] D–H \cdots A	Symmetry operations
Boc-(L-Leu-L-Leu-Aib) ₂ -L-Leu-D-Leu-Aib-OMe (2)					
	N ₄ –H	O ₀	3.47 ^{b)}	156	<i>x, y, z</i>
	N ₅ –H	O ₁	2.91	165	<i>x, y, z</i>
	N ₆ –H	O ₂	3.20	161	<i>x, y, z</i>
	N ₇ –H	O ₄	3.01	134	<i>x, y, z</i>
	N ₈ –H	O ₅	2.89	163	<i>x, y, z</i>
	N ₉ –H	O ₄	3.01	163	<i>x, y, z</i>
	N ₁ –H	O _D ^{a, c)}	2.90	140	<i>x, 1+y, z</i>
	N ₂ –H	O _{7'}	2.81	162	<i>x, 1+y, z</i>
Boc-L-Leu-D-Leu-Aib-L-Leu-L-Leu-Aib-L-Leu-D-Leu-Aib-OMe (3)					
Molecule A					
	N _{4a} –H	O _{0a}	3.14	165	<i>x, y, z</i>
	N _{5a} –H	O _{1a}	2.89	160	<i>x, y, z</i>
	N _{6a} –H	O _{2a}	3.09	165	<i>x, y, z</i>
	N ₇ –H	O _{3a}	3.18	149	<i>x, y, z</i>
	N _{8a} –H	O _{5a}	2.94	163	<i>x, y, z</i>
	N _{9a} –H	O _{4a}	2.93	163	<i>x, y, z</i>
Molecule B					
	N _{4b} –H	O _{0b}	3.25	163	<i>x, y, z</i>
	N _{5b} –H	O _{1b}	2.95	161	<i>x, y, z</i>
	N _{6b} –H	O _{2b}	3.02	169	<i>x, y, z</i>
	N _{7b} –H	O _{3b}	3.31 ^{b)}	148	<i>x, y, z</i>
	N _{8b} –H	O _{5b}	2.99	159	<i>x, y, z</i>
	N _{9b} –H	O _{4b}	2.95	141	<i>x, y, z</i>
	N _{1b} –H	O _M ^{c)}	2.85	154	<i>x, y, z</i>
	N _{2b} –H	O _{7a}	2.74	122	<i>x, y, z</i>
	O _M –H ^{c)}	O _{6a}	2.74	166	<i>x, y, z</i>
	N _{3a} –H	O _{7b'}	3.04	157	$-1+x, -1+y, z$

a) The amino acid numbering of the residues begins at the N-terminus of the peptide chain. b) The D \cdots A distance is a bit long for a hydrogen bond. c) O_D: DMA, O_M: MeOH.

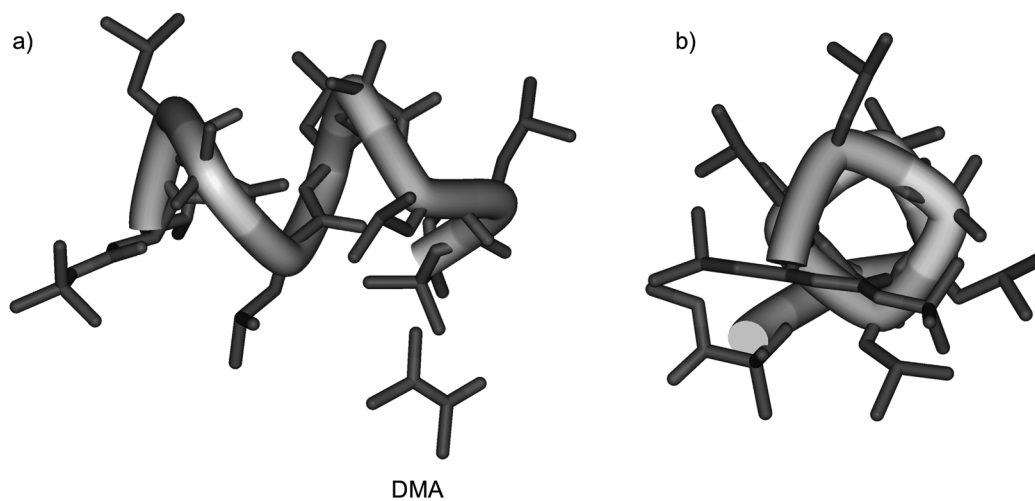


Fig. 4. X-Ray Diffraction Structure of the Nonapeptide 2 as Viewed (a) Perpendicular to and (b) along Its Helical Axis

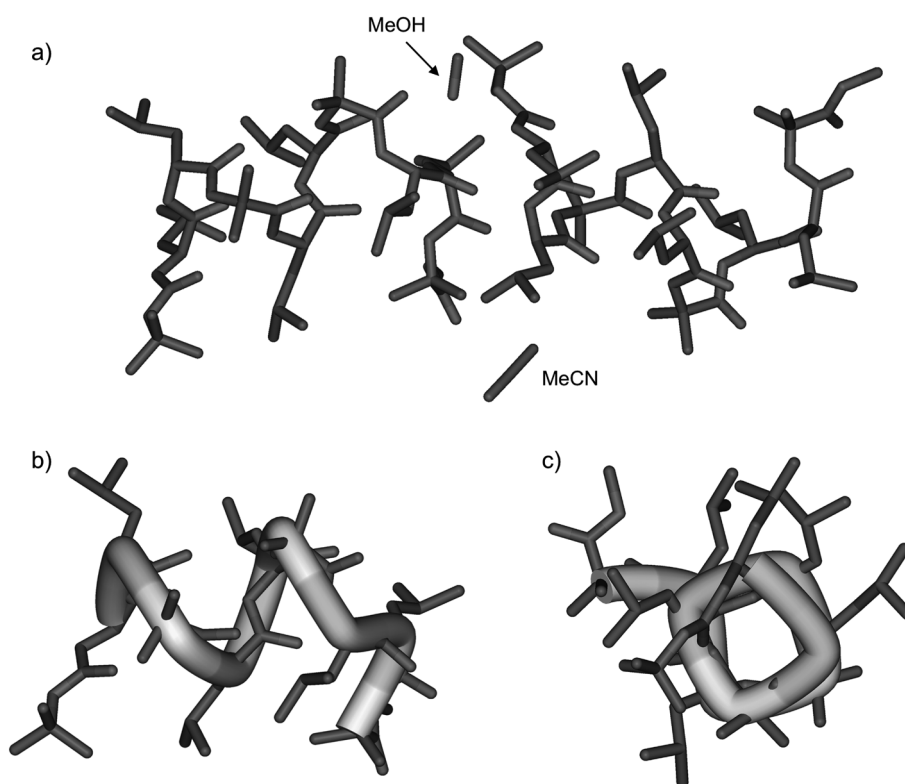


Fig. 5. X-Ray Diffraction Structure of the Nonapeptide 3 as Viewed (a) Perpendicular to and (b) along Its Helical Axis

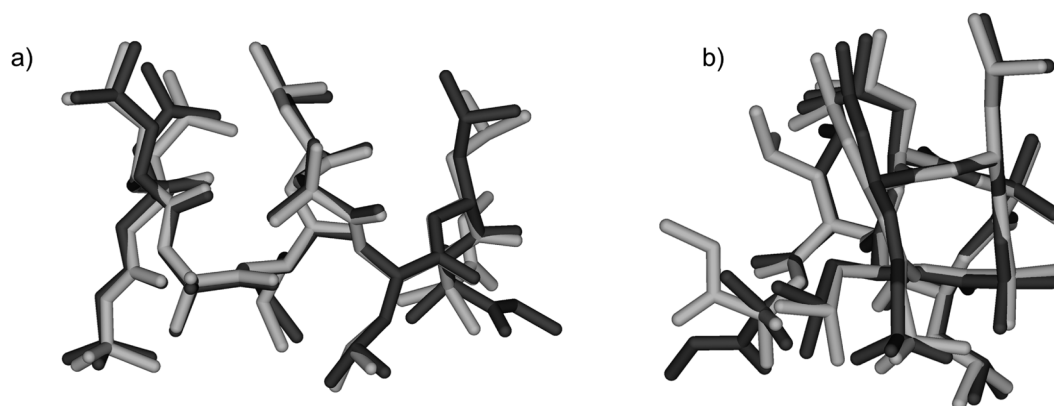


Fig. 6. Superimposed Structures of Molecules A (Light Gray) and B (Gray) as Viewed (a) Perpendicular to and (b) along Their Helical Axes

[N(8b)···O(5b)=2.99 Å], and between the H-N(9b) and C(4b)=O(4b) [N(9b)···O(4b)=2.95 Å]. In packing mode, molecules **A** and **B** were alternately connected by intermolecular hydrogen bonds.

Conclusion

Four diastereomeric nonapeptides, Boc-(L-Leu-L-Leu-Aib)₃-OMe (**1**),¹³ Boc-(L-Leu-L-Leu-Aib)₂-L-Leu-D-Leu-Aib-OMe (**2**), Boc-L-Leu-D-Leu-Aib-L-Leu-L-Leu-Aib-L-Leu-D-Leu-Aib-OMe (**3**), and Boc-(L-Leu-D-Leu-Aib)₃-OMe (**4**),¹⁴ were synthesized to investigate the influence of D-Leu residues on the helical structures of L-Leu-based nonapeptides. In solution, the homochiral peptide **1**, which only contained L-Leu residues, formed the most right-handed (*P*) helical structure. Increasing the number of D-Leu residues in the L-Leu-based nonapeptide sequence decreased the right-handedness of the resultant helical peptides. Peptides **1**, **2**, and **3** formed 3₁₀-helices as their dominant conformations, whereas the dominant conformation of peptide **4**, which contained alternating L-Leu-D-Leu fragments, was an α -helix. In short peptide sequences, Aib residues are able to stabilize 3₁₀-helices, but not α -helices, and therefore, peptides **1**, **2**, and **3** formed 3₁₀-helices in solution. On the other hand, peptide **4**, which was composed of the well-regulated L-Leu-D-Leu-Aib segment, formed a right-handed (*P*) α -helix rather than a 3₁₀-helix.¹⁵

In the crystalline state, peptide **2**, which contained one D-Leu residue, and peptide **3**, which contained two D-Leu residues, were folded into (*P*) α -helices with flipped C-terminal D-Leu (8) residues. In packing mode, peptides **3** and **4** probably tend to form α -helices, rather than 3₁₀-helices, in order to avoid amino acid side-chain competition between the *i* and *i*+3 positions. The incorporation of increasing numbers of D-Leu residues into L-Leu-based helical nonapeptides gradually destabilizes the right-handedness of their helices and tends to change their dominant conformations from 3₁₀-helices to α -helices. These findings could have important implications for the construction of well-defined short helical peptides.

Experimental

General Optical rotation $[\alpha]_D$ was assessed using a 1.0 dm cell in MeOH. ¹H- and ¹³C-NMR spectra were recorded at 400 MHz and 100 MHz in CDCl₃ using tetramethylsilane as an internal standard. Fourier transform infrared (FT-IR) spectra were recorded on a JASCO FT/IR-4100 spectrometer at a resolution of 1 cm⁻¹ over a mean of 128 scans using the solution (CDCl₃) method and NaCl cells with a path length of 0.1 mm. CD spectra were recorded with a JASCO J-720W spectropolarimeter using a cell with a 1.0-mm path length. The resultant data are expressed in terms of $[\theta]_R$, the total molar ellipticity (deg cm² dmol⁻¹). 2,2,2-Trifluoroethanol (TFE) and a mixture of TFE/PBS (1:1) solution were used as a solvent. The data collection for the X-ray diffraction analysis was performed on Rigaku RAXIS-RAPID and Bruker AXS SMART APEX imaging plate diffractometers using graphite-monochromated MoK α radiation.

Boc-(L-Leu-L-Leu-Aib)₂-L-Leu-D-Leu-Aib-OMe (2) Colorless crystals; mp 225–227°C; $[\alpha]_D^{21} = -11.8$ (*c*=0.5, CHCl₃); IR (ATR): ν 3434, 3334, 2961, 2871, 1736, 1662 cm⁻¹; ¹H-NMR (400 MHz, CDCl₃) δ : 7.74 (d, *J*=6.0 Hz, 1H), 7.58 (d, *J*=7.6 Hz, 1H), 7.55 (brs, 1H), 7.31 (d, *J*=6.0 Hz, 1H), 7.25 (br s, 1H), 7.13 (br s, 1H), 7.10 (d, *J*=8.0 Hz, 1H), 6.77 (brs, 1H),

5.44 (brs, 1H), 4.30–4.41 (m, 2H), 3.80–4.11 (m, 4H), 3.68 (s, 3H), 1.39–1.88 (m, 45H), 0.79–1.00 (m, 36H); ¹³C-NMR (100 MHz, CDCl₃) δ : 176.3, 175.6, 175.2, 175.1, 174.6, 173.7, 173.4, 173.0, 175.2, 81.9, 57.4, 57.1, 55.9, 55.7, 55.3, 55.1, 54.9, 52.6, 52.4, 40.6, 40.4, 40.1, 40.0, 39.4, 28.5, 27.6, 27.2, 25.7, 25.4, 25.3, 25.2, 25.1, 24.7, 23.8, 23.5, 23.4, 23.3, 23.0, 22.2, 21.9, 21.7, 21.6, 21.1, 21.0; [high resolution electrospray ionization (HR-ESI)(+)]: *m/z* Calcd for C₅₄H₉₉N₉O₁₂Na [M+Na]⁺ 1088.7311; found 1088.7313.

Boc-L-Leu-D-Leu-Aib-L-Leu-L-Leu-Aib-L-Leu-D-Leu-Aib-OMe (3) Colorless crystals; mp 237–239°C; $[\alpha]_D^{21} = +2.2$ (*c*=0.5, CHCl₃); IR (ATR): ν 3439, 3334, 2960, 2871, 1735, 1662 cm⁻¹; ¹H-NMR (400 MHz, CDCl₃) δ : 7.60–7.71 (m, 4H), 7.51 (brs, 1H), 7.43 (brs, 1H), 7.23 (brs, 1H), 7.18 (brs, 1H), 5.59 (brs, 1H), 4.20–4.32 (m, 2H), 4.08 (m, 1H), 3.98 (m, 1H), 3.84 (m, 1H), 3.73 (m, 1H), 3.67 (s, 3H), 1.40–1.96 (m, 45H), 0.78–1.09 (m, 36H); ¹³C-NMR (100 MHz, CDCl₃) δ : 176.7, 175.8, 175.5, 174.9, 174.8, 173.9, 173.3, 172.8, 157.1, 81.5, 57.6, 57.3, 56.1, 55.9, 55.2, 55.1, 53.9, 53.3, 53.0, 52.6, 40.9, 40.1, 39.7, 39.5, 38.0, 28.8, 27.9, 27.0, 25.9, 25.5, 25.2, 25.1, 24.9, 24.0, 23.7, 23.6, 23.5, 23.1, 22.3, 22.0; [HR-ESI(+)]: *m/z* Calcd for C₅₄H₉₉N₉O₁₂Na [M+Na]⁺ 1088.7311; found 1088.7309.

Acknowledgments This study was supported, in part, by JSPS KAKENHI Grant No. 26460169 (Y.D.) and by a Grant-in-Aid from the Tokyo Biochemical Research Foundation (Y.D.).

Conflict of Interest The authors declare no conflict of interest.

References and Notes

- 1) Crisma M., Formaggio F., Moretto A., Toniolo C., *Biopolymers Peptide Science*, **84**, 3–12 (2006).
- 2) Royo S., Borggraefe W. M., Peggion C., Formaggio F., Crisma M., Jiménez A. I., Cativiela C., Toniolo C., *J. Am. Chem. Soc.*, **127**, 2036–2037 (2005).
- 3) Demizu Y., Doi M., Kurihara M., Maruyama T., Suemune H., Tanaka M., *Chemistry*, **18**, 2430–2439 (2012).
- 4) Demizu Y., Misawa T., Kurihara M., *J. Synth. Org. Chem. Jpn.*, **18**, 2430–2439 (2012).
- 5) Gellman S. H., *Acc. Chem. Res.*, **31**, 173–180 (1998).
- 6) Cheng R. P., Gellman S. H., DeGrado W. F., *Chem. Rev.*, **101**, 3219–3232 (2001).
- 7) Seebach D., Beck A. K., Bierbaum D. J., *Chem. Biodivers.*, **1**, 1111–1239 (2004).
- 8) Goodman C. M., Choi S., Shandler S., DeGrado W. F., *Nat. Chem. Biol.*, **3**, 252–262 (2007).
- 9) Imamura Y., Umezawa N., Osawa S., Shimada N., Higo T., Yokoshima S., Fukuyama T., Iwatsubo T., Kato N., Tomita T., Higuchi T., *J. Med. Chem.*, **56**, 1443–1454 (2013).
- 10) Blackwell H. E., Sadowsky J. D., Howard R. J., Sampson J. N., Chao J. A., Steinmetz W. E., O'Leary D. J., Grubbs R. H., *J. Org. Chem.*, **66**, 5291–5302 (2001).
- 11) Kim Y.-W., Grossmann T. N., Verdine G. L., *Nat. Protoc.*, **6**, 761–771 (2011).
- 12) Demizu Y., Tanaka M., Nagano M., Kurihara M., Doi M., Maruyama T., Suemune H., *Chem. Pharm. Bull.*, **55**, 840–842 (2007).
- 13) Demizu Y., Doi M., Kurihara M., Okuda H., Nagano M., Suemune H., Tanaka M., *Org. Biomol. Chem.*, **9**, 3303–3312 (2011).
- 14) Demizu Y., Doi M., Sato Y., Tanaka M., Okuda H., Kurihara M.,

- Chem. Eur. J.*, **17**, 11107–11109 (2011).
- 15) Demizu Y., Yamashita H., Yamazaki N., Sato Y., Doi M., Tanaka M., Kurihara M., *J. Org. Chem.*, **78**, 12106–12113 (2013).
- 16) Crisma M., Bonora G. M., Toniolo C., Benedetti E., Bavoso A., Di Blasio B., Pavone V., Pedone C., *Int. J. Biol. Macromol.*, **10**, 300–304 (1988).
- 17) Toniolo C., Polese A., Formaggio F., Crisma M., Kamphuis J., *J. Am. Chem. Soc.*, **118**, 2744–2745 (1996).
- 18) Sheldrick G. M., “Program for Crystal Structure Refinement (SHELXL 97),” University of Göttingen, Göttingen, 1997.
- 19) Beurskens P. T., Admiraal G., Beurskens G., Bosman W. P., De Gelder R., Israel R., Smits J. M. M., “The DIRDIF-99 program system,” Technical Report of the Crystallography Laboratory, University of Nijmegen, the Netherlands, 1994.
- 20) CCDC-993731 for **2**, CCDC-855722 for **3**, contain the supplementary crystallographic data for this paper. These data can be obtained free of charge from The Cambridge Crystallographic Data Centre. <http://www.ccdc.cam.ac.uk/data_request/cif>
- 21) Schellman C., “Protein Folding,” Elsevier/North-Holland, New York, 1980, pp. 53–61.
- 22) Aravinda S., Shamala N., Bandyopadhyay A., Balaram P., *J. Am. Chem. Soc.*, **125**, 15065–15075 (2003).